**JOURNAL OF AERONAUTICS AND SPACE TECHNOLOGIES**
(ISSN : 1304-0448)
January 2019 Volume 12 Number 1
www.jast.hho.edu.tr

**Research Article**

# A Wideband Square Spiral Antenna for Multiple Airborne Applications

Cihan DÖĞÜŞGEN ERBAŞ[1], Ali OKATAN[2]

[1] *Istanbul Yeni Yuzyil University, Istanbul, Turkey,* cihan.dogusgen@yeniyuzyil.edu.tr,
[2] *Istanbul Gelisim University, Istanbul, Turkey* aokatan@gelisim.edu.tr

**Article Info**

***Received:*** *August 13, 2018*
***Accepted:*** *November 19, 2018*
***Online:*** *January 23, 2019*

**Keywords:** Airborne Application, Balun, Square Spiral Antenna, Wideband Antenna, Wideband Impedance Matching.

**Abstract**

In this article, we designed a wideband square spiral antenna with an impedance matching part that operated between 1500 – 5500 MHz (covering L, S, and C bands) for airborne uses such as Aeronautical Mobile Satellite Service, radar altimeters, Microwave Landing System, and airborne weather radars. The impedance matching part was a designed wideband balun. We obtained simulation results for scattering parameters, radiation patterns, antenna and system input impedances and gain values. The results confirmed that the antenna showed good matching and radiation characteristics within the mentioned frequency range.

**To Cite This Article:** C. D. Erbas, , A. Okatan, "A Wideband Square Spiral Antenna for Multiple Airborne Applications" Journal of Aeronautics and Space Technologies, Vol 12, No. 1, pp. 31-40, Jan. 2019.

# Çoklu Hava Uygulamaları İçin Bir Geniş Bantlı Karesel Sarmal Anten

**Makale Bilgisi**

***Geliş:*** *13 Ağustos 2018*
***Kabul:*** *19 Kasım 2018*
***Yayın:*** *23 Ocak 2019*

**Anahtar Kelimeler:** Hava Uygulamaları, Balun, Karesel Sarmal Anten, Geniş Bantlı Anten, Geniş Bantlı Empedans Uydurma.

**Öz**

Bu makalede, Hava Mobil Uydu Servisi, radar altimetreleri, Mikrodalga İniş Sistemi ve hava radarları gibi hava aracı üzerinde taşınan kullanımlar için 1500-5500 MHz (L, S, ve C bantlarını kapsayan) aralığında çalışan, bir empedans uydurma kısmına sahip bir geniş bantlı karesel sarmal anten tasarladık. Empedans uydurma kısmı, tasarlanmış bir geniş bantlı balun idi. Saçılma parametreleri, ışıma örüntüleri, anten ve sistem giriş empedansları ile kazanç değerleri için benzetim sonuçlarını elde ettik. Sonuçlar, antenin bahsedilen frekans aralığında iyi uyumlandırma ve ışıma karakteristikleri gösterdiğini doğrulamıştır.

## 1. INTRODUCTION

A number of communication and navigation systems as well as landing aids in different frequency bands are present on an aircraft. The systems operating in L, S and C bands include Aeronautical Mobile Satellite System (AMSS), radar altimeters (RAs), Microwave Landing System (MLS), and airborne weather radars (AWRs).

AMSS relays data from air to ground through a satellite via available channels [1]. AMSS downlink and uplink frequency bands are between 1525-1559 MHz, and 1626.5-1660.5 MHz, respectively. RAs measure the height of the aircraft above terrain immediately below the aircraft. RAs operate within a frequency range of 4200-4400 MHz. MLS is an all- weather landing system that replaced the former Instrument Landing System (ILS) for aircraft. It operates in C band between 5031-5090 MHz. AWRs provide weather detection through the reflectivity of water droplets. AWR operation band is between 5350-5470 MHz.

An aircraft needs to establish several links for its communications, and therefore airborne antennas are required to receive and transmit different signals. Moreover, wideband antennas have been of interest in communication technologies such as data and voice communication, multimedia, surveillance, and telemetry because it is important to handle different applications with a compact single antenna. Various wideband antenna topologies for airborne applications have been reported in literature: Ramirez and Santos [2] designed and optimized an irregularly shaped microstrip patch antenna for air-to-ground communications. The final antenna resonated at 14250 MHz with a 10 dB bandwidth of 3700 MHz. The antenna had significantly lower radiation levels in the boresight direction in $\phi$=0$^{O}$ plane, and the gain values were not presented Sairam et. al. [3] proposed a monopole blade antenna for airborne usage covering 500-2000 MHz. The radiating element was the union of a planar square and a triangle printed on RT Duroid 5880 substrate. They obtained a VSWR lower than 3:1 for the whole bandwidth. Compared to our proposed structure, that antenna had a lower bandwidth, and was taller with a height of 95 mm, which made the antenna larger-size. Thain et. al. [4] reported various dual band phased array elements based on broadband patch antenna technology for civil aviation applications. The final structure operated in both L-band and Ku band. The radiation pattern was weak in low elevation angles for one designed antenna, as stated in their article. Furthermore, performance of another designed antenna was not presented.

Archimedean spiral antennas are one type of wideband antennas that have received a significant amount of attention over the past several decades due to their reasonably compact and low profile dimensions, stable input impedance as well as symmetrical radiation pattern characteristics [5,6]. Circular and square/rectangular Archimedean spiral antennas are commonly used. In order to obtain smaller antennas with similar performances, square/rectangular Archimedean spiral antennas are preferable. Various research has been conducted to examine these antennas [7-10].

One of the main challenges in Archimedean spiral antenna design is wideband impedance matching. In general, an Archimedean spiral antenna has an input impedance not less than 90 ohms [11], which means that an impedance transformer is needed between the spiral and 50-ohm input. For two arm spirals, previous researchers proposed several typical feeding methods, including the infinite balun that was presented by Dyson [5], the vertical coaxial line to parallel line balun [6], and the latest modified Dyson-style balun [7, 8].

In this study, we presented a two-arm wideband square spiral antenna with an exponentially tapered balun for wideband matching to 50 ohms. The structure operated between 1500 – 5500 MHz. We provided design steps for the antenna and the impedance matching part along with simulation results of scattering parameters, radiation patterns, and input impedances. We carried out the simulations through Ansoft HFSS. The designed structure had a significantly wider 10 dB bandwidth, which was 4000 MHz, compared to the antennas in the cited studies. The radiation levels were higher, and provided suitable coverage in all directions. Value for the gain, an important parameter in antenna design, was also high at a selected frequency.

## 2. ANTENNA

The designed antenna was a two-arm square Archimedean spiral antenna. We used theoretical equations for circular spiral antennas, and optimized the square spiral antenna geometry to obtain the final configuration.

We utilized Equation (1), which stated the relation between the lowest frequency of operation ($f_L$) and outer radius of the antenna ($R_{out}$) for a circular spiral antenna

$$f_L = \frac{c}{2\pi R_{out}} \quad (1)$$

where c=3.10$^{8}$ m/sec was the speed of light, and $f_L$=1500 MHz for our case. Resulting $R_{out}$ was 31.83 mm.

Likewise, Equation (2) related the highest frequency of operation ($f_H$) and inner radius of the antenna ($R_{in}$) for a circular spiral antenna:

$$f_H = \frac{c}{2\pi R_{in}} \quad (2)$$

where $f_H$=5500 MHz, and resulting $R_{in}$=8.68 mm.

We calculated the width of spiral arm ($w$), and the spacing between the spiral arms through Equation (3):

$$s = w = \frac{R_{out} - R_{in}}{4N} \quad (3)$$

in which $N$ was the number of of turns. We set $N$=13 throughout the design. We calculated $s$ and $w$ as 0.45 mm.

We initially simulated the square spiral antenna structure by using the computed parameters above. Then we optimized the design, which yielded final values for half-diagonal of the spiral, distance from spiral center to first turn of the spiral along the diagonal, and width of the spiral arm as 44.86 mm, 4.44 mm and 0.777 mm, respectively. The distance between the two spiral arms aligned through the origin was 2 mm. We determined this parameter by taking into account the balun design, which is given in the following section.

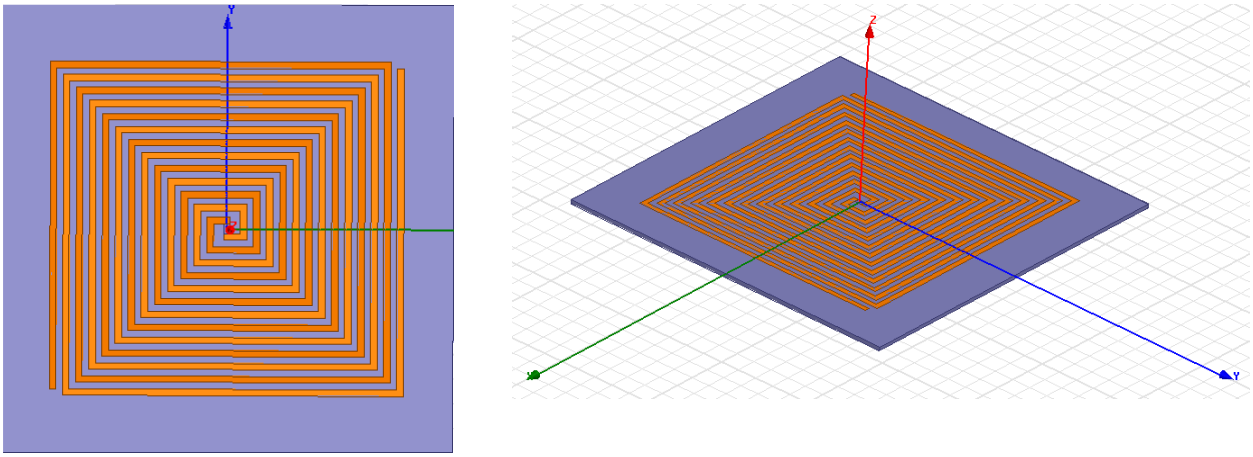


(a) (b)

**Figure 1.** Square spiral antenna printed on duroid substrate: (a) Top view (b) Side view.

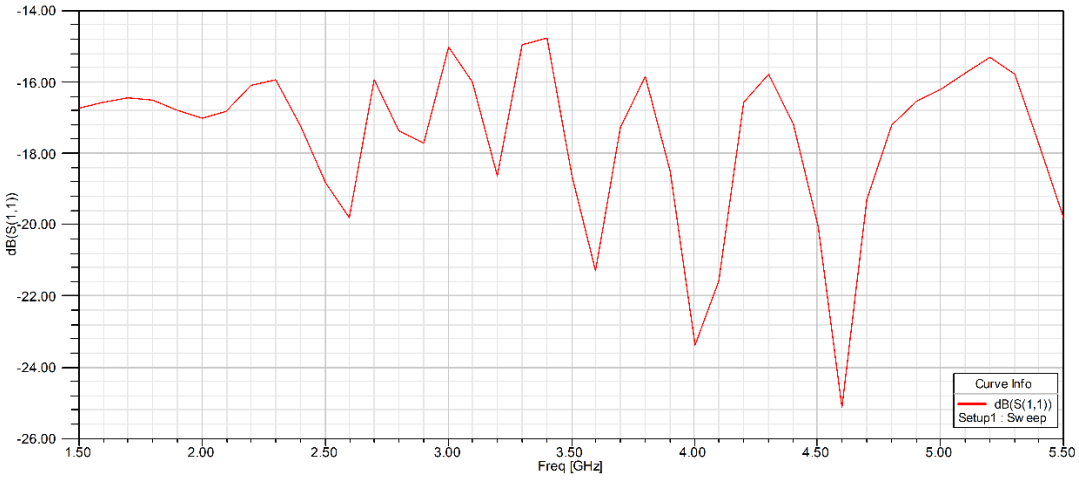


**Figure 2.** Scattering parameter $S_{11}$ versus frequency for the square spiral antenna.

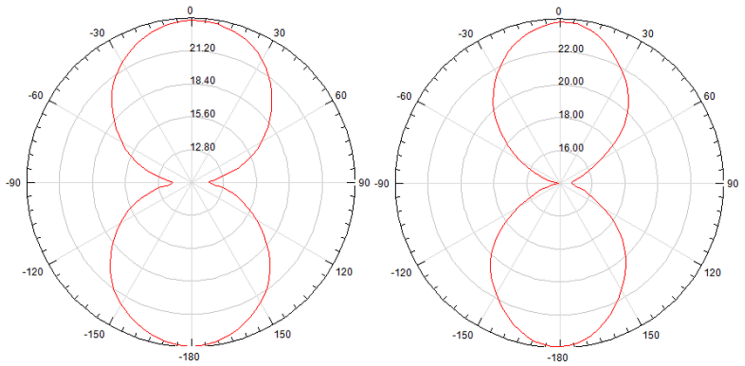


(a) (b)

**Figure 3.** Radiation patterns for the antenna at $f$=3.5 GHz: (a) $\phi$=0$^O$ plane (b) $\phi$=90$^O$ plane.

The antenna was printed on a square duroid substrate with a relative permittivity of 2.2 and a loss tangent of 0.0009. The substrate area and height were 90x90 mm$^2$ and 1 mm, respectively. The antenna was free-standing, and we did not take into account the ground plane effect because the designed balun would be connected to the antenna. During the simulations, it was centrally fed by a lumped port with a reference impedance of 188 ohms, a typical value for the input impedance of Archimedean spiral antennas. Figure 1 shows the antenna geometry.

Figure 2 depicts the scattering parameter $S_{11}$ for the antenna against frequency. $S_{11}$ variation was clearly well below -10 dB for the entire bandwidth between 1500 – 5500 MHz. Figure 3 illustrates the radiation patterns of the antenna at $f$=3500 MHz, mid-frequency of the frequency band, for $\phi$=0$^O$ and $\phi$=90$^O$ planes. We obtained bi-directional radiation patterns for both planes. Figure 4 shows the real and imaginary parts of the antenna input impedance, which were relatively stable within the bandwidth of interest, before impedance matching. Maximum simulated gain at 3500 MHz was 6.22 dBi.

We observed consecutive resonant frequencies as illustrated in Figure 2 and Figure 4. That was because the planar spiral antenna operated as a resonator having multiple resonance modes. The observed modes were analogous to the TEM modes of an open circuited transmission line resonator [12]. Few studies have investigated the higher order resonances in spiral antennas: Maleeva et. al. [12] suggested an analytical method to calculate the mode frequencies for one-arm, circular spiral antennas with inner radii approaching the outer radii (i.e. the thin spiral limit). Hooker et. al. [13] presented a more general analytical method that applied to one-arm, circular spiral antennas. As far as known, there was no study that had investigated two-arm, square spiral antennas in order to analytically compute the higher order resonant frequencies. To compute the first resonant frequency in our case, we considered the spiral antenna as a center-fed half-wavelength transmission line, which satisfied the open-circuit boundary condition at the line ends. However, the analytical and simulation results were inconsistent. We also applied the approach in [13], and obtained unmatched results. We concluded that the analytical calculation of the first and higher order resonant frequencies of two-arm, square spiral antennas required further research.

## 3. IMPEDANCE MATCHING PART

We aimed to match the antenna input impedance (assumed to be 188 ohms, which was a typical value for Archimedean spiral antennas) to 50 ohms for the frequency band of interest. To do that, we designed an exponentially tapered microstrip transmission line to obtain a wideband balun. The tapered microstrip structure consisted of two tapered strips printed on both sides of a duroid substrate with a relative permittivity of 2.2 and a loss tangent of 0.0009.

Considering a substrate height of $h$, and a signal strip width of $w$, the characteristic impedance of a microstrip line ($Z_0$) was [14,15].

$$Z_0 = \begin{cases} \frac{60}{\sqrt{\varepsilon_{eff}}} \ln\left(\frac{8h}{w} + \frac{w}{4h}\right) & if\ \frac{w}{h} < 1 \\ \frac{120\pi}{\sqrt{\varepsilon_{eff}}\left(\frac{w}{h} + 1.393 + 0.667 ln\left(\frac{w}{h} + 1.444\right)\right)} & if\ \frac{w}{h} > 1 \end{cases} \quad (4)$$

where

$$\varepsilon_{eff} = \frac{\varepsilon_r + 1}{2} + \frac{\varepsilon_r - 1}{2\sqrt{1 + 12h/w}} \quad (5)$$

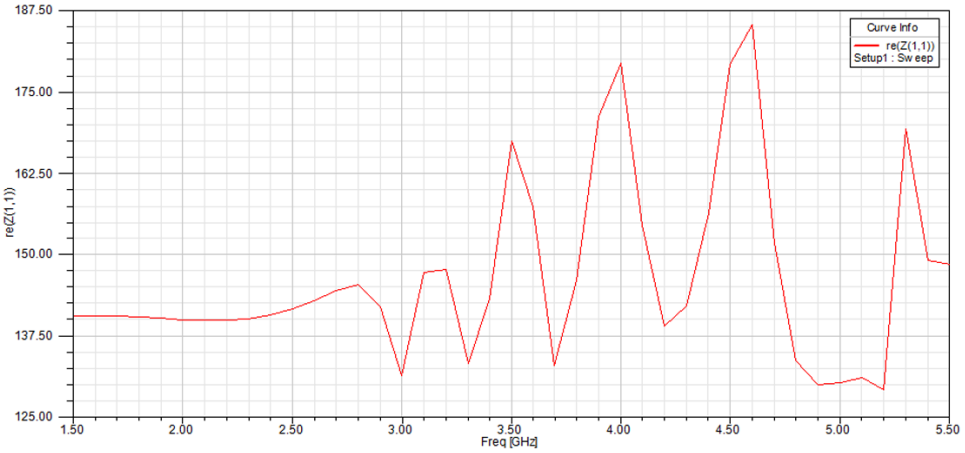


(a)

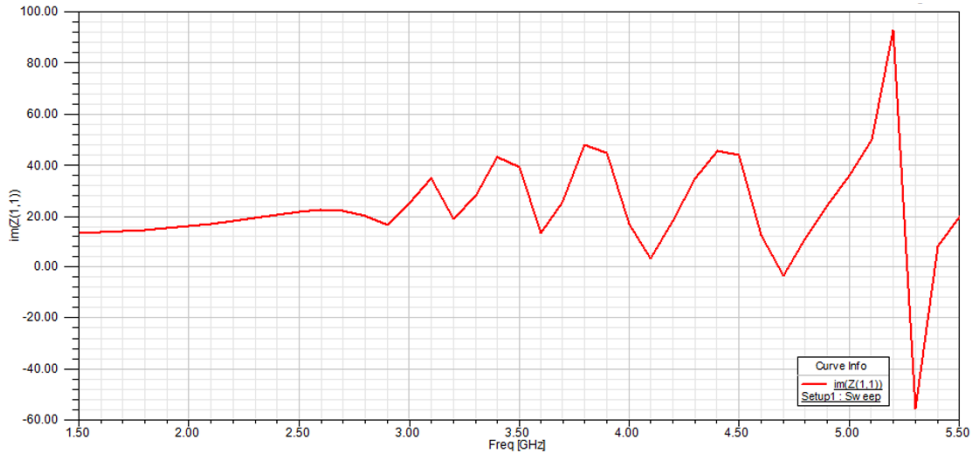


(b)

**Figure 4.** Antenna input impedance versus frequency before impedance matching: (a) Real part (b) Imaginary part.

was the effective dielectric constant. We used Equations (4)-(5) to design the top layer of the balun. For the bottom layer of the balun, we optimized the dimensions through HFSS. Figure 5 shows the both layers.

We defined $h$=2 mm. The top and ground layers of the balun were printed on both sides of the substrate. Value of the chosen $h$ was the same as the distance between the two spiral arms (aligned through the origin) of the designed square spiral antenna, as indicated in the previous section. We placed the balun between these two spiral arms so that the top and ground layers of the balun were connected to the spiral antenna.

We chose the total length of the tapered line as $L$=40 mm. Then we divided the tapered line into 8 parts with individual characteristic impedances between 50 ohms and 188 ohms. Through Equations (4)-(5), we extracted $w$ for each part for known $Z_0$ and $h$.

In order to compute the position of each part along $L$, we utilized the following equation for the exponential taper:

$$Z(z) = Z_0 e^{\alpha z} \tag{6}$$

where $Z(z)$ and $\alpha$ were the output characteristic impedance of each part along $z$ axis and an exponential coefficient, respectively. First, we determined $\alpha$=33.111 by substituting $Z(z)$=188 ohms, $Z_0$=50 ohms, and $z$=$L$=0.04 m. Using the evaluated $\alpha$ value, and $Z_0$=50 ohms, we extracted $z$ for the previously determined characteristic impedance profile. Table 1 illustrates the widths for the top and bottom layers of balun as well as the position of each part along $L$. Figure 6 depicts the scattering parameter $S_{11}$ versus frequency for the designed balun. For the whole frequency band of interest, $S_{11}$ was below -10 dB.

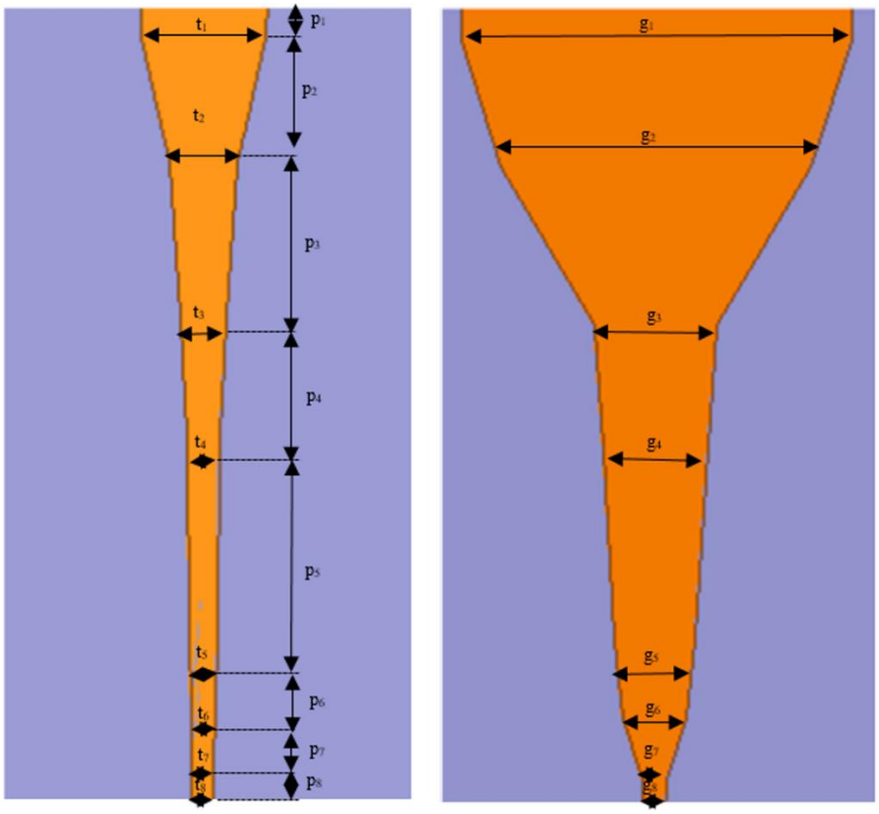


(a) (b)

**Figure 5.** (a) Top layer widths (denoted by t) and positions (denoted by p) (b) Ground layer widths (denoted by g). Note that top and ground layer positions are the same.

**Table 1.** Characteristic impedance, top layer width, ground layer width, and position profile.

| Characteristic impedance (ohm) | $Z_{01}$=50 | $Z_{02}$=70 | $Z_{03}$=90 | $Z_{04}$=110 | $Z_{05}$=150 | $Z_{06}$=170 | $Z_{07}$=188 | $Z_{08}$=188 |
|---|---|---|---|---|---|---|---|---|
| Top width (mm) | $t_{1}$= 6.096 | $t_2$= 3.302 | $t_3$= 2.2352 | $t_4$=1.524 | $t_5$=1.397 | $t_6$=1.1684 | $t_7$=1.1176 | $t_8$=1.1176 |
| Ground width (mm) | $g_1$=19 | $g_2$=15 | $g_3$=6 | $g_4$=5.1 | $g_5$=3.9 | $g_6$=3.1 | $g_7$=1.1176 | $g_8$=1.1176 |
| Position (mm) | $p_1$=2 | $p_2$=6.2 | $p_3$=7.6 | $p_4$=6.0 | $p_5$=9.4 | $p_6$=3.8 | $p_7$=3.0 | $p_8$=2.0 |

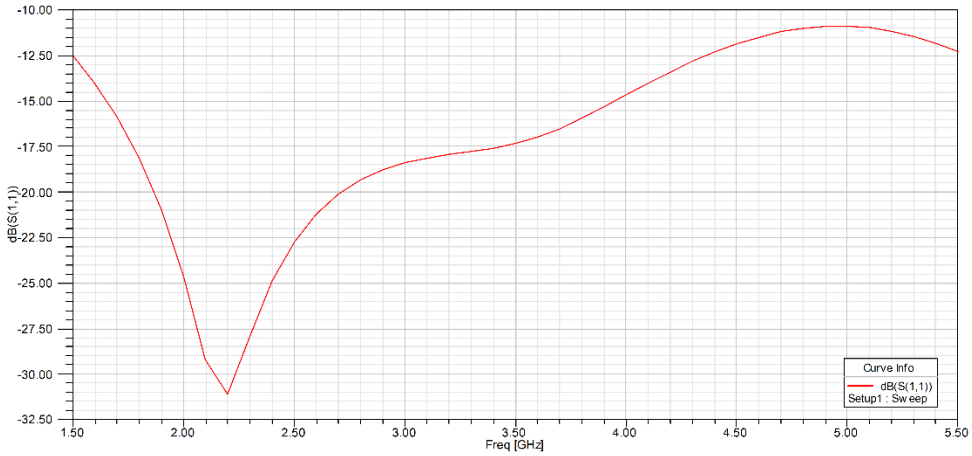


**Figure 6.** Scattering parameter $S_{11}$ versus frequency for the wideband balun.

## 4. ANTENNA WITH IMPEDANCE MATCHING PART

After designing the square spiral antenna and the impedance matching wideband balun, we combined these two parts together to obtain the final configuration, as illustrated in Figure 7. Figure 8 shows the scattering parameter $S_{11}$ for the whole structure as a function of frequency. The scattering parameter $S_{11}$ remained below -10 dB threshold within the frequency band of interest. Input impedance of the combined antenna and wideband balun was relatively stable, and was close to 50 ohms in the entire band, as given in Figure 9. Note that during the simulations, the final configuration was fed by a lumped port with a reference impedance of 50 ohms applied between the ground layer and top layer of the balun. The feed was located at the middle of the balun end with the largest ground and top layer widths. Figure 10 depicts the radiation patterns of the final configuration at $f$=3500 MHz for $\phi$=0$^O$ and $\phi$=90$^O$ planes. We observed bi-directional radiation patterns for both planes without significant degradation compared to the sole antenna radiation patterns. Maximum simulated gain at 3500 MHz was 6.06 dBi, which indicated that the degradation in maximum gain was insignificant compared to the sole antenna. The structure was elliptically polarized with an axial ratio larger than 3 dB within the frequency band of interest.

## 5. CONCLUSIONS

We developed a two-arm wideband square spiral antenna with an impedance matching wideband balun for several airborne applications such as AMSS, RA, MLS, and AWR. The structure operated between 1500-5500 MHz covering L, S and C bands. We provided the design steps for both the square spiral antenna and the impedance matching part. The scattering parameter $S_{11}$ was below -10 dB for the antenna and the impedance matching part as well as the combined structure. We lowered the input impedance of the antenna close to 50 ohms after impedance matching. The antenna and the combined structure presented bi-directional radiation patterns. Furthermore, degradation in the radiation patterns of the combined structure for both $\phi$=0$^O$ and $\phi$=90$^O$ planes was insignificant compared to the sole square spiral antenna. In the future, we could consider including a radome to protect the system from outer environment, and evaluate its impacts on the simulation results.

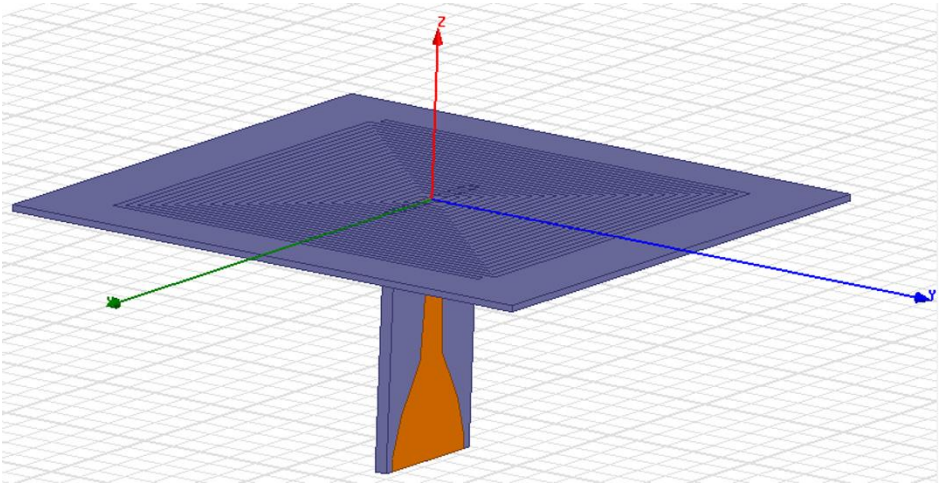


**Figure 7.** Combined antenna and wideband balun geometry.

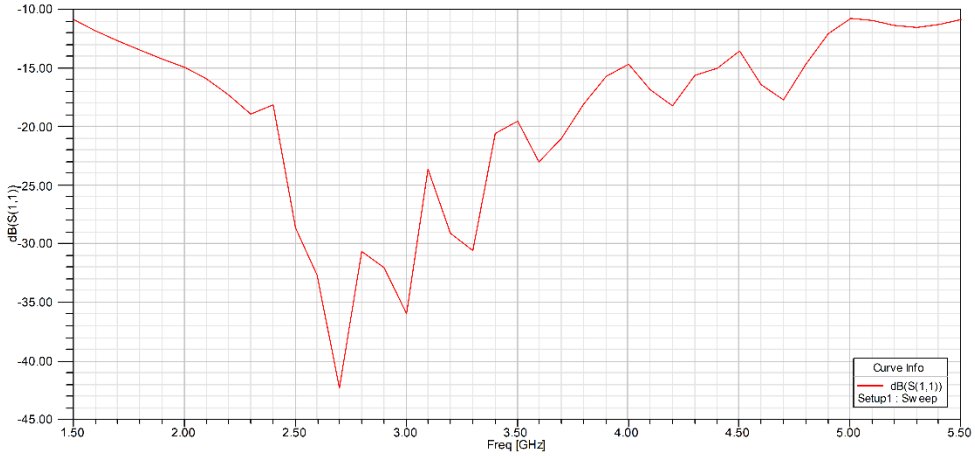


**Figure 8.** Scattering parameter $S_{11}$ versus frequency for the antenna and wideband balun combined together.

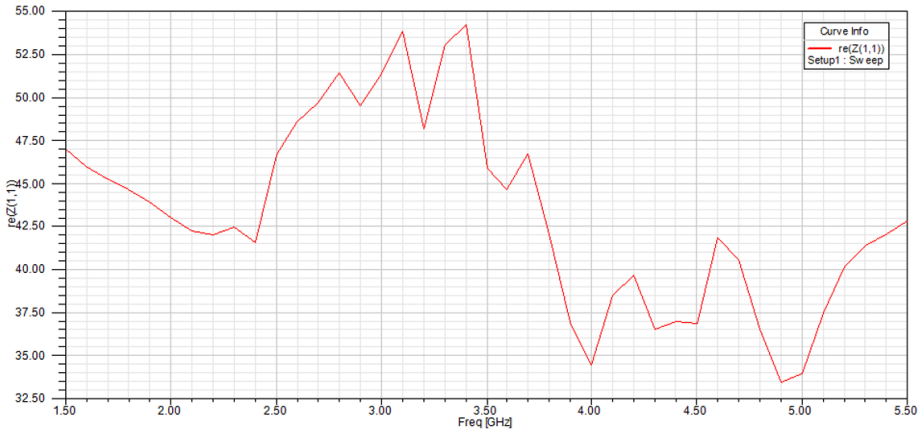


(a)

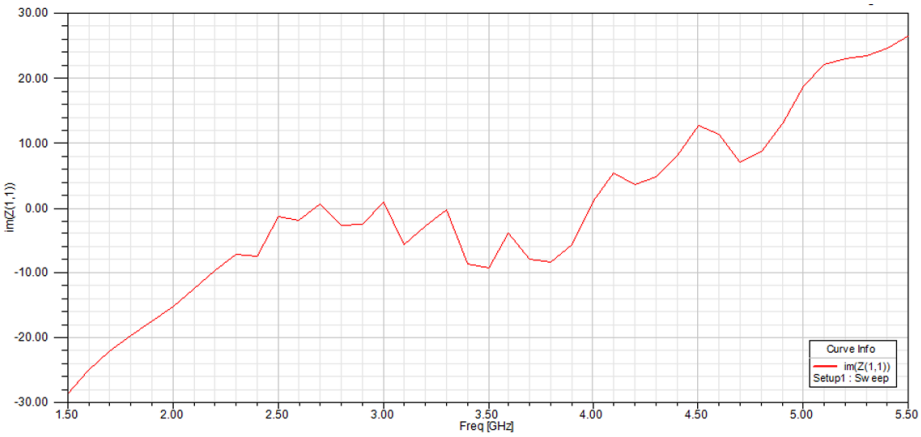


(b)

**Figure 9.** Input impedance of the combined antenna and wideband balun versus frequency: (a) Real part (b) Imaginary part.

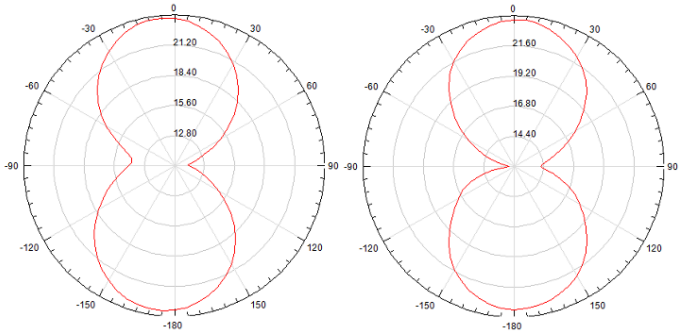

(a) (b)

**Figure 10.** Radiation patterns at f=3.5 GHz: (a) $\phi$=0$^{O}$ plane (b) $\phi$=90$^{O}$ plane.

## 6. REFERENCES

**[1]** Ripamonti, C., Konangi, V. K., Kerozewski, R. J., "Simulation and performance of data communication using AMSS," *In: IEEE Aerospace Conference*, pp. 1177-1181, 2002.

**[2]** Ramirez, L. A. R., Santos J. C. A., "Design, simulation, and optimization of an irregularly shaped microstrip patch antenna for air-to-ground communications," *International Journal of Antennas and Propagation*, Vol. 2017, pp. 1-9, 2017.

**[3]** Sairam, C., Khumanthem, T., Ahirwar, S., Singh, S., "Broadband blade antenna for airborne applications," *In: Annual IEEE India Conference-Engineering Sustainable Solutions*, pp. 1-4, 2011.

**[4]** Thain, A., Peres, G., Hulzinga, A., Schippers, H., et. al., "A dual-band low profile phased array antenna for civil aviation applications," *In: IEEE 3rd European Conference on Antennas and Propagation*, pp. 1337-1341, 2009.

**[5]** Shih, T. Y., Behdad, N., "A compact, broadband, spiral antenna with unidirectional circularly polarized radiation patterns," *IEEE Transactions on Antennas and Propagation*, Vol. 63, No. 6, pp. 2776-2781, 2015.

**[6]** Fang, H. R., Serhir, M., Guinvarch, R., Mouthaan, K., "Enhanced dual-circular polarised four-arm Archimedean spiral antenna with low-profile cavity backing," *IET Microwaves, Antennas & Propagation*, Vol. 9, pp. 1260-1266, 2015.

**[7]** Goudos, S. K., Siakavara, K., Sahalos, J. N., "Design of load-ended spiral antennas for RFID UHF passive tags using improved artificial bee colony algorithm," *International Journal of Electronics and Communications (AEÜ)*, Vol. 69, pp. 206-214, 2014.

**[8]** Wei, H., Lin, M., Xiang, Y., "Compact square spiral printed antenna," *Electronics Letters*, Vol. 50, No. 3, pp. 135-136, 2014.

**[9]** Zhang, X., Han, Y., Li, W., Duan, X., "A rectangular planar spiral antenna for GIS partial discharge detection," *International Journal of Antennas and Propagation*, Vol. 2014, pp. 1-7, 2014.

**[10]** Lee, J. H., Seo, D. W., Lee, H. S., "Design of implantable rectangular spiral antenna for wireless biotelemetry in the MICS band," *ETRI Journal*, Vol. 37, No. 2, pp. 204-211, 2015.

**[11]** Li, D., Li, L., Li, Z., Ou, G., "Four-arm spiral antenna fed by tapered transmission line," *IEEE Antennas and Wireless Propagation Letters*, Vol. 16, pp. 62-65, 2017.

**[12]** Maleeva, N., Fistul, M. V., Karpov, A., Zhuravel, A. P., et. al., "Electrodynamics of a ring-shaped spiral resonator," *Journal of Applied Physics*, Vol. 115, No. 6, pp. 1-25, 2014.

**[13]** Hooker, J. W., Ramaswamy, V., Arora, R. K., Edison, A. S., et. al., "An empirical expression to predict the resonant frequencies of Archimedean spirals," *IEEE Transactions on Microwave Theory and Techniques*, Vol. 63, No. 7, 2107-2114.

**[14]** Vinayagamoorthy, K., "Design and implementation of wideband baluns for Archimedean spiral antennas," *MS Thesis*, 54, 2011.

**[15]** Bahl, I. J., Trivedi, D. K., "A designer' s guide to microstrip lines," *Microwaves*, pp. 174-182, 1977.

## VITAE

**Assistant Prof. Dr. Cihan Doguşgen Erbas** was born in Istanbul, Turkey in 1979. She received her B.S. and M.Sc. degrees in Electronics and Communication Engineering from Technical University of Istanbul in 2001 and 2003, respectively. Then she was awarded her Ph.D. degree in Electrical Engineering from Iowa State University, Ames, Iowa, USA in 2009. She is currently an assistant professor of Electrical and Electronics Engineering at Istanbul Yeni Yuzyil University, Turkey. Her research interests include antenna design, microwave radiometry, synthetic aperture radar data processing, and electromagnetic compatibility problems.

**Prof. Dr. Ali Okatan** was born in Turkey in 1950. He completed his B. S. and M.Sc. in the the fields of Electrical Engineering at Technical University of Istanbul, Turkey (1973). Prof. Okatan has completed his Ph. D. in Electrical Engineering at Iowa State University, Ames, Iowa, USA (1977). Dr. Okatan has many research, papers, books and projects in electronics, computer systems and nuclear physics. He is a member of IEEE, Sigma Xi, Cern Alice. Now, he is vice rector and head of computer engineering Department at Istanbul Gelişim University.